

### Publication III

N. Chekurov, K. Grigoras, A. Peltonen, S. Franssila, and I. Tittonen. 2009. The fabrication of silicon nanostructures by local gallium implantation and cryogenic deep reactive ion etching. *Nanotechnology*, volume 20, number 6, 065307, 5 pages.

© 2009 Institute of Physics Publishing (IOPP)

Reprinted by permission of Institute of Physics Publishing.

# The fabrication of silicon nanostructures by local gallium implantation and cryogenic deep reactive ion etching

N Chekurov<sup>1,2</sup>, K Grigoras<sup>1,2</sup>, A Peltonen<sup>2,3</sup>, S Franssila<sup>1,2</sup> and I Tittonen<sup>1,2</sup>

<sup>1</sup> Department of Micro and Nanosciences, Helsinki University of Technology, PO Box 3500, FI-02015 TKK, Finland

<sup>2</sup> Center for New Materials, Helsinki University of Technology, PO Box 3500, FI-02015 TKK, Finland

<sup>3</sup> TKK Micronova, Helsinki University of Technology, PO Box 3500, FI-02015 TKK, Finland

E-mail: [nikolai.chekurov@tkk.fi](mailto:nikolai.chekurov@tkk.fi)

Received 17 October 2008, in final form 26 November 2008

Published 14 January 2009

Online at [stacks.iop.org/Nano/20/065307](http://stacks.iop.org/Nano/20/065307)

## Abstract

We show that gallium-ion-implanted silicon serves as an etch mask for fabrication of high aspect ratio nanostructures by cryogenic plasma etching (deep reactive ion etching). The speed of focused ion beam (FIB) patterning is greatly enhanced by the fact that only a thin approx. 30 nm surface layer needs to be modified to create a mask for the etching step. Etch selectivity between gallium-doped and undoped material is at least 1000:1, greatly decreasing the mask erosion problems. The resolution of the combined FIB-DRIE process is 20 lines  $\mu\text{m}^{-1}$  with the smallest masked feature size of 40 nm. The maximum achieved aspect ratio is 15:1 (e.g. 600 nm high pillars 40 nm in diameter).

## 1. Introduction

Focused ion beam milling and etching (with reactive gas in addition to the ion beam) are established micro- and nanofabrication techniques [1, 2]. Fabrication of deep 3D structures requires very high ion doses, in the range of  $10^{18} \text{ cm}^{-2}$ . On the other hand, 2D surface patterning, which depends on local modification and damage injection, can be done with fairly low doses,  $10^{12}$ – $10^{15} \text{ cm}^{-2}$  for modification of a few nanometer thick surface layers [3].

Schmidt *et al* [4] have shown that gallium-beam-treated silicon is resistant towards plasma etching. This was attributed to approx. 10 nm thick gallium oxide layer formation in  $\text{SF}_6/\text{O}_2$  plasma. However, no etching of micro- or nanostructures was demonstrated. Qian *et al* [5] demonstrated a fabrication method where microstructures were etched using gallium-implanted silicon as a mask in RIE. They reported only low aspect ratio structures with micrometer dimensions.

In the work of Robinson [6] alumina thin film was treated by FIB to create an ordered array of 100 nm diameter pores. These FIB-treated areas were used as initial pits for the electrochemical pore formation, and consequently these alumina pores acted as masks for argon ion milling of silicon.

High density of nanopores was demonstrated ( $10^{11} \text{ cm}^{-2}$ ) but no other types of structures were made. Compared with self-organized nanopore formation, the FIB-created initial pits led to a uniform hexagonal hole array. Also a square-grid array was fabricated which is not possible utilizing self-organized pore formation.

Top surface imaging [7] is a well-known lithography technique where a thin imaging layer is placed on top of a thicker resist layer which is responsible for the etch resistance, while the thin top layer is designed for high resolution patterning only. This technique has been extended from optical to focused ion beam lithography [8]. Gallium was implanted into a thin surface layer of resist, and oxygen plasma treatment was utilized to transform this Ga-implanted layer into gallium oxide, which then acted as an etch mask for the subsequent oxygen plasma development step. After those masking procedures, the process is continued in a conventional way with a thick resist acting as an etch/implant mask.

In this work we show that the gallium implantation method can be extended to high aspect ratio 3D nanostructures with 40 nm as the smallest feature size. The etch rate ratio (selectivity) between gallium-implanted and non-implanted

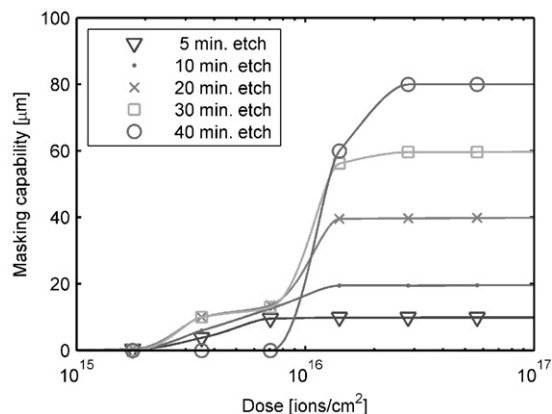


**Figure 1.** Obtained step height versus gallium dose. Flattening of the curve corresponds to the etch-resistant mask. Various curves represent various DRIE etch times.

silicon enables deep plasma etching (more than 80  $\mu\text{m}$ ) as well as high aspect ratios up to 15:1. One novelty of the proposed technique is in its writing speed. The combination of FIB surface layer modification with cryogenic DRIE enables dramatic writing time reductions in nanostructure fabrication. Also the sidewall control is easier with DRIE than with FIB milling/etching.

## 2. $\text{Ga}^+$ masking dose and selectivity

The experiments with the local implantation were performed using a Helios Nanolab 600 dual-beam system (FEI Company). A liquid metal source is used to generate a  $\text{Ga}^+$  ion beam with currents between 1.5 pA and 22 nA. The dwell time can be varied between 50 ns and 4.6 ms. The ion energy was kept at 30 keV which in silicon produces an ion range of 28 nm with a straggle of 10 nm. The maximum field of view, which determines the largest writable structure, is approx.  $700 \times 700 \mu\text{m}^2$ . This whole area can be modified into an etch-resistant state in less than 17 min using the maximum ion current.

The DRIE etching experiments were carried out in a Plasmalab System 100 reactor (Oxford Instruments). The system has two power sources: high density  $\text{SF}_6/\text{O}_2$  plasma is generated by an inductively coupled plasma (ICP) source at 13.56 MHz and ion energies are controlled separately with a capacitively coupled plasma (CCP) source operating also at 13.56 MHz. The wafer is cooled down to  $-120^\circ\text{C}$  by a liquid-nitrogen-cooled electrode. Mechanical clamping of the wafer and the backside cooling by helium ensure the effective heat exchange between the cooled electrode and the wafer. The etching parameters were varied to produce optimal results. The ICP power range was 800–1000 W, CCP power 2–3 W and  $\text{SF}_6/\text{O}_2$  flows were 40/6–6.5 sccm.

XPS analyses were performed using an AXIS 165 electron spectrometer (Kratos Analytical). All data was acquired using monochromatic Al radiation at 100 W.

In order to study  $\text{Ga}^+$  ion dose effect on etch resistance, eight ( $300 \mu\text{m} \times 300 \mu\text{m}$ ) square areas were irradiated with ion doses ranging from  $10^{15}$  to  $10^{17} \text{cm}^{-2}$ . Irradiated samples were

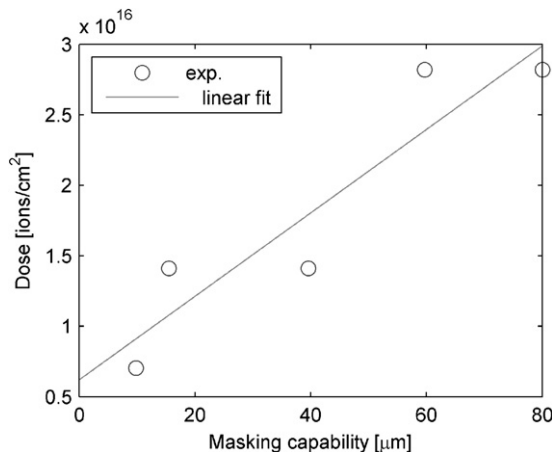


**Figure 2.** Minimum  $\text{Ga}^+$  doping dose to gain the etch resistance that is sufficient for the fabrication of structures of a given depth.

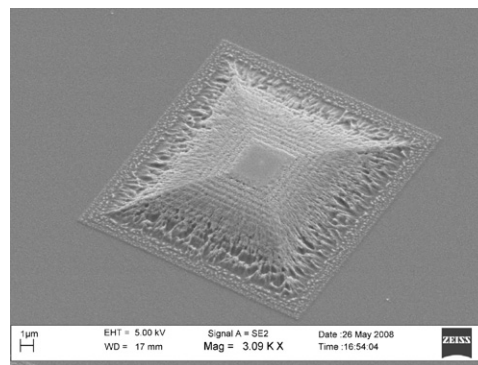


**Figure 3.** 3D structure created in a single 1 min etch step by using 20 linearly increasing doses from  $1.75 \times 10^{14} \text{cm}^{-2}$  (at rim) to  $3.5 \times 10^{15} \text{cm}^{-2}$  (at central square area). The height of the resulting structure is 1.6  $\mu\text{m}$ .

etched for various time intervals and the heights of the resulting structures were measured. The rather large size of these test structures allows us to neglect the effect of the shape of the ion beam and the ion distribution pattern, as the beam diameter is much smaller than the treated area (1/1000). Knowing the beam current and irradiation time, the ion dose in the center of the test structure can be accurately calculated. In figure 1 the heights of the etched silicon structures are plotted against the gallium dose for various etch times. One can conclude that a threshold value of  $2 \times 10^{15} \text{cm}^{-2}$  is needed before any etch resistance is achieved, and eventually by applying a dose of  $2 \times 10^{16} \text{cm}^{-2}$ , very high etch resistance follows. We project a maximum etched depth of at least 80  $\mu\text{m}$  with a dose of  $3 \times 10^{16} \text{cm}^{-2}$ , as shown in figure 2. The thickness of the  $\text{Ga}^+$ -doped region is approximated to be 50 nm, yielding a selectivity of over 1500:1 between treated and untreated silicon.

Dose-dependent mask resistance allows us to create three-dimensional objects in a single etch step as shown in figure 3. The largest shown square area was doped with a dose of  $1.75 \times 10^{14} \text{cm}^{-2}$ . The following square-shaped dopings were performed on top of each other using the same dose, so the

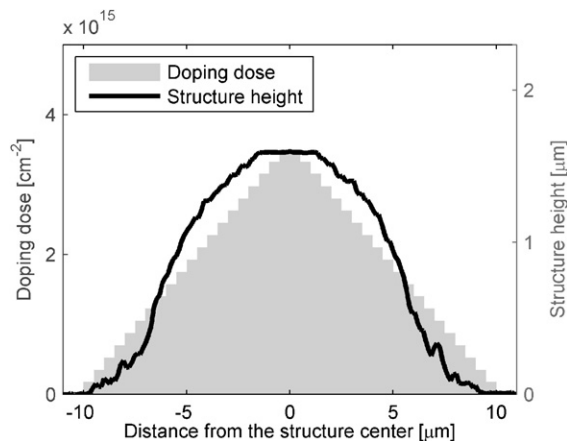


**Figure 4.** Ga<sup>+</sup> doping dose chart and the height of the resulting structure: dose steps and the corresponding AFM-measured step heights after 1 min etch.

smallest of the 20 square-shaped areas was finally doped to the maximum dose of  $3.5 \times 10^{15} \text{ cm}^{-2}$ . The structure was etched for 1 min producing the maximum height of  $1.6 \mu\text{m}$ .

The doping profile as well as the resulting structure height is shown in figure 4. The steps on the structure are formed due to the mask failure and etching of the material underneath. The plateau on top of the pyramid is an indication that the heavily doped masking layers in the center of the structure did not fail during etching. With doses less than  $1.7 \times 10^{15} \text{ cm}^{-2}$  the masking becomes non-uniform, protecting some areas more efficiently than others and creating a rough surface. We suspect this to be because of statistical variation in the dose, leading to pinhole defects which initiate the silicon etching.

To determine the mechanism behind the masking effect of the Ga<sup>+</sup> dopant, chemical compositions of surfaces of a series of samples were analyzed using x-ray photoelectron spectroscopy (XPS). The series consisted of four silicon samples which were doped to approximately  $3 \times 10^{16} \text{ cm}^{-2}$ . The first one was left unetched, serving as a reference sample. The second piece was etched for 10 s with SF<sub>6</sub>/O<sub>2</sub> plasma, the third one was treated for the same time with SF<sub>6</sub> plasma without oxygen and the last sample was etched in SF<sub>6</sub>/O<sub>2</sub> mixture for 5 min.

As seen from XPS analysis (figure 5) the unetched sample contained no gallium in the top surface layer, as expected from simulations. In all etched samples, irrespective of the etch time and etch gas composition, 6–8 at.% of gallium was detected. This indicated that etching of silicon proceeds until gallium concentration rises and starts to act as an etch stop. Even a 5 min long extended etch (sample 4) did not significantly alter the gallium surface concentration. The results are summarized in table 1. Oxygen and fluorine are both present on the surface of all samples. Both gallium oxide and gallium fluoride are non-volatile and could be responsible for the etch stop.

### 3. Determination of resolution

The FIB-DRIE process can be used to create arbitrary mask patterns in silicon for structures in the 100 nm range as shown

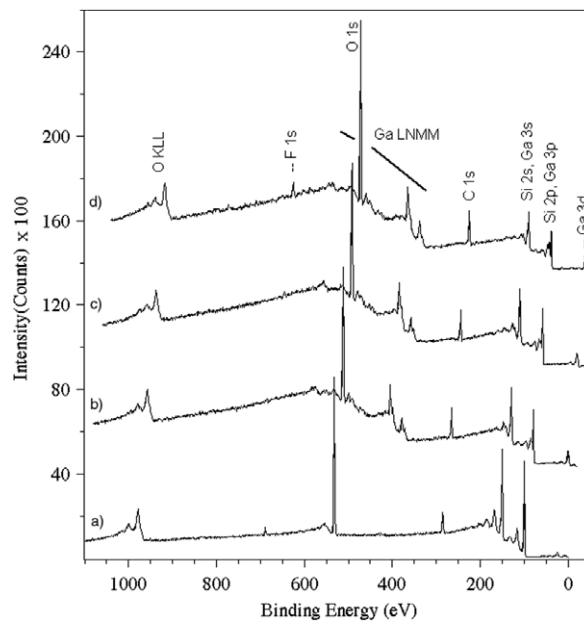


**Figure 5.** The result of the XPS measurements. (a) Unetched sample, (b) sample etched with SF<sub>6</sub>/O<sub>2</sub> plasma for 10 s, (c) sample etched with SF<sub>6</sub> only for 10 s and (d) sample etched with SF<sub>6</sub>/O<sub>2</sub> plasma for 5 min.

**Table 1.** Summary of the XPS analyses. The samples were doped with gallium to a dose of  $3 \times 10^{16} \text{ cm}^{-2}$  and etched with various plasma compositions.

	F (%)	Ga (%)	Si (%)	C (%)	O (%)
Unetched (a)	1	0	47	14	37
SF <sub>6</sub> /O <sub>2</sub> 10 s (b)	2	8	22	25	44
SF <sub>6</sub> 10 s (c)	1	8	23	22	47
SF <sub>6</sub> /O <sub>2</sub> 5 min (d)	3	6	16	25	52

in figure 6. The sidewall profile of the pillars is nearly vertical and the uniformity across the array excellent. Below 100 nm the non-idealities of the DRIE process will limit the minimum size of nanostructures. The high rate of the cryogenic SF<sub>6</sub>/O<sub>2</sub> etching process exhibits an undercut of the mask of the order of 20 nm, regardless of the geometry of the structure. Figures 6(a) and (b) show silicon nanopillars 280 nm in diameter and 4 μm in height, with a minor undercut. The undercut plays a more prominent role with the smaller structures (figure 6(c)). Undercutting can be reduced at the expense of etch rate, and by optimizing the DRIE process for the reduction of the undercut one can produce pillar-type nanostructures that are even smaller than 50 nm in diameter.

By fabricating a sequence of various stripes and spaces (figure 7), the minimum linewidth was measured to be 54 nm (initially 47 nm on a mask) and the narrowest trench is 43 nm (50 nm on a mask). The widening of the written structures is approximately 7 nm and the resolution of the process is 20 lines μm<sup>-1</sup>.

The most demanding application of this fabrication method is to create nanopillars which are as narrow as possible, but still with high aspect ratio. While it is relatively straightforward to create very small single structures (figure 8),

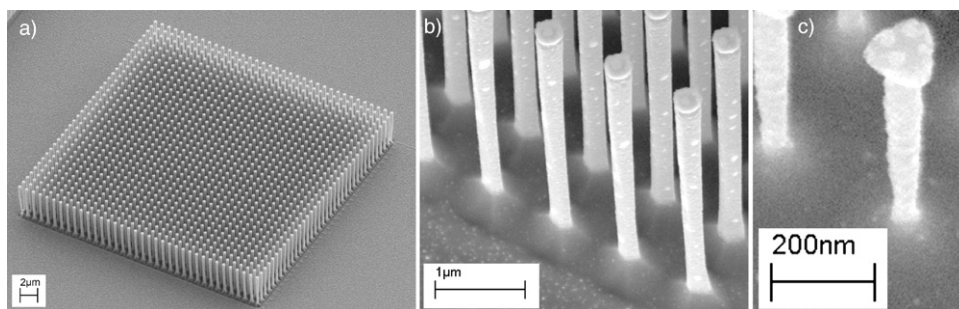


**Figure 6.** (a) Pillars with 280 nm diameter after DRIE (3 min etch time) in a high density  $36 \times 36$  array, (b) close-up view of the array, (c) a 600 nm high (30 s etch time) pillar with a diameter of 65 nm, demonstrating the undercut of the triangular masking layer: the micrographs are taken at  $30^\circ$  inclination.

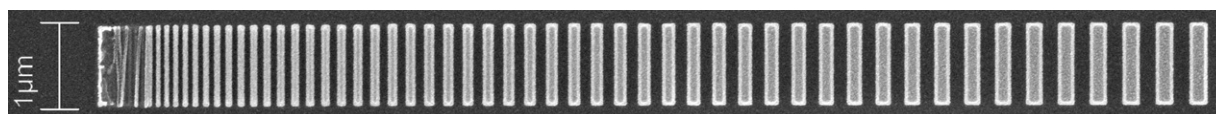


**Figure 7.** Variation of the width (7–310 nm) of the line-shaped structures. The narrowest reproducible line is 54 nm.

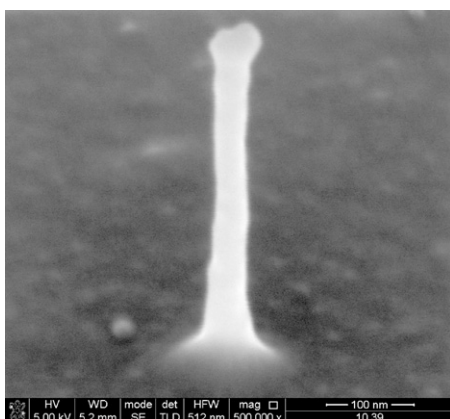


**Figure 8.** Single pillar 40 nm in diameter and 600 nm tall.

dense matrices require good repeatability and act as a much more stringent test for the fabrication method.

Figure 9 shows a test structure for determining the maximum array density. The minimum structure diameter obtained in this kind of formation is 85 nm with a 200 nm pitch.

#### 4. Conclusion

FIB is an excellent tool for nanofabrication because of its patterning flexibility and its additional capability of even inclined structuring. However, its processing speed is seriously limited. Even in gas-assisted mode the capability to mill large area structures or high pattern density structures is poor. Our approach of using FIB in surface modification rather than as a 3D structuring tool offers orders of magnitude improvement in writing speed. The writing speed is proportional to the current used, which can be chosen over a wide range according to the particular application in question. With the lowest current (1.5 pA) it will take 0.5 ms to protect a single spot which is 20 nm in diameter. Larger areas can be filled by a broad, high

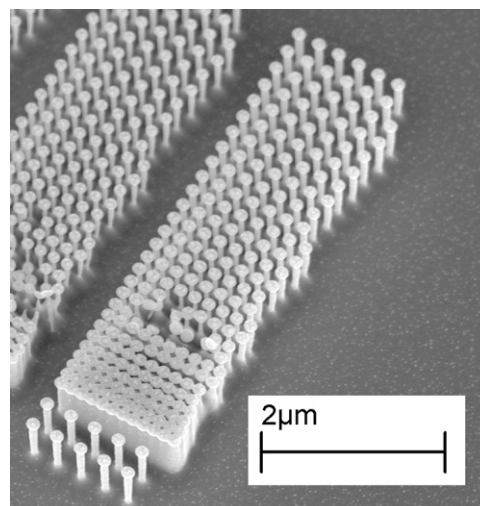


**Figure 9.** 84 nm wide and 600 nm tall pillars in a matrix of variable density with the minimum pitch of 200 nm.

current beam. The maximum writable area for the FIB used is  $700 \times 700 \mu\text{m}^2$ . Structures that are this large can be made etch-resistant in about 17 min using 21 nA current. Direct milling of an area of this size only for 100 nm depth will take approximately 250 min and creating structures in the range of tens of micrometers high is not feasible.

Extension of the gallium modification technique to dark-field patterns, such as holes and trenches, is ongoing. We expect to see similar types of improvements in fabricating even much more complex three-dimensional shapes.

This fabrication method enables the creation of silicon structures down to a few tens of nanometers in size and is not limited to any specific patterns. Together with the full processing time of only a few hours and with the absence of any wet processing steps, the method can greatly speed up the prototyping phase in nanotechnology.

## Acknowledgments

Lauri Sainiemi is acknowledged for discussions on DRIE mask material effects. We acknowledge Drs Leena-Sisko Johansson and Joseph Campbell from The Forest Products Surface Chemistry Group at TKK Department of the Forest Products Technology for the XPS analyses. NC thanks the Magnus Ehrnrooth Foundation for financial support.

## References

- [1] Reytjens S and Puers R 2001 *J. Micromech. Microeng.* **11** 287
- [2] Tseng A 2004 *J. Micromech. Microeng.* **14** R15
- [3] Gierak J *et al* 2005 *Microelectron. Eng.* **78/79** 266
- [4] Schmidt B, Oswald S and Bischoff L 2005 *J. Electrochem. Soc.* **152** G875
- [5] Qian H X, Zhou W, Miao J, Lim L E N and Zeng X R 2008 *J. Micromech. Microeng.* **18** 035003
- [6] Robinson A P, Burnell G, Hu M and MacManus-Driscoll J L 2007 *Appl. Phys. Lett.* **91** 143123
- [7] Satou I, Watanabe M, Watanabe H and Itani T 2000 *Japan. J. Appl. Phys.* **39** 6966
- [8] Arshak K, Mihov M, Nikahara S, Arshak A and McDonagh D 2005 *Microelectron. Eng.* **78/79** 39